



CHEMISTRY

A European Journal

A Journal of



Accepted Article

Title: Host-host Interactions Control Self-assembly and Switching of Triple and Double Decker Stacks of Tricarbazole Macrocycles Co-assembled with Anti-electrostatic Bisulfate Dimers

Authors: James Robert Dobscha, Sibali Debnath, Rachel Elizabeth Fadler, Elisabeth Maria Fatila, Maren Pink, Krishnan Raghavachari, and Amar H. Flood

This manuscript has been accepted after peer review and appears as an Accepted Article online prior to editing, proofing, and formal publication of the final Version of Record (VoR). This work is currently citable by using the Digital Object Identifier (DOI) given below. The VoR will be published online in Early View as soon as possible and may be different to this Accepted Article as a result of editing. Readers should obtain the VoR from the journal website shown below when it is published to ensure accuracy of information. The authors are responsible for the content of this Accepted Article.

To be cited as: *Chem. Eur. J.* 10.1002/chem.201800827

Link to VoR: <http://dx.doi.org/10.1002/chem.201800827>

Supported by
ACES

WILEY-VCH

Host-host Interactions Control Self-assembly and Switching of Triple and Double Decker Stacks of Tricarbazole Macrocycles Co-assembled with *Anti*-electrostatic Bisulfate Dimers

James R. Dobscha^a, Sibali Debnath^a, Rachel E. Fadler^a, Elisabeth M. Fatila^{a,b}, Maren Pink^a, Krishnan Raghavachari^a, Amar H. Flood^{a*}

^a Department of Chemistry, Indiana University, 800 E. Kirkwood Avenue, Bloomington, IN 47405, USA.

^b Current address: Department of Chemistry, Louisiana Tech University, 1 Adams Boulevard, Ruston, LA 71272, USA.

Accepted Manuscript

ABSTRACT

Hierarchical assembly provides a route to complex architectures when using building blocks with strong and structurally well-defined recognition elements. These rules are expressed using cationic templates with reliable metal-ligand bonding but use of anions is rare on account of weak anion-host contacts. We investigate an approach that relies on host-host interactions to fortify assemblies formed between bisulfate anion dimers, $[\text{HSO}_4\cdots\text{HSO}_4]^{2-}$, and shape-persistent macrocycles called tricarbazole triazolophanes. These macrocycles have significant self-association. In chloroform, they form high fidelity, triple-decker stacks with bisulfate dimers. The strength of host-host interactions allows for preferential formation of the 3:2 tricarb:bisulfate architecture over an ion-paired architecture seen with analogous macrocycles with much weaker self-association. Solvent was expected and found to tune host-host contacts enabling formation of a 2:2 complex and solvent-driven switching between triple- and double- stacked structures. Crystallography of the 2:2:2 complex supports the idea that significant host-host interactions with tricarb arises from dipole-stabilized π -stacking. Computational studies were also conducted further highlighting the importance of host-host interactions in stacked complexes of tricarb. These findings unambiguously verify the importance of host-host interactions in the assembly and stability of discrete, responsive anion-templated architectures.

Introduction

The multi-component, hierarchical assembly of molecular building blocks^[1] is of interest for the preparation of discrete and environmentally responsive architectures.^[2] These structures are characterized by reliable design rules: strong inter-component contacts with well-defined geometries. For example, tetrahedra,^[3] cubes,^[4] and nanospheres^[5] all utilize strong metal-ligand binding^[6] with preferred stereochemistries. Anion-directed assemblies are rarer^[7] and often emerge as the after-effect of cation-directed assembly.^[8] Their rarity can be attributed to weaker anion-host binding. New strategies for assembly are needed to overcome this problem. Helicates^[9] and tetrahedra^[10] use anions of higher charge (2-/3-),^[9e-g, 10] leverage polydentate hosts,^[9a-c, 9e-g, 10] or use non-coordinating cations.^[9a-c, 9e-g, 10] New anion-directed self-assembly has been seen with hydroxyanions like bisulfate (HSO_4^-) and hydrogen phosphate (H_2PO_4^-) that also display these features. These anions form *anti*-electrostatic,^[11] self-complementary $\text{OH}\cdots\text{O}$ hydrogen bonds (Figure 1a)^[12] to become linked together and raise their charge,^[13] such as bisulfate dianion dimers $[\text{HSO}_4\cdots\text{HSO}_4]^{2-}$.^[14] These dimers are stabilized in solution when co-assembled with a host,^[15] e.g., cyanostar macrocycles.^[14, 16] Yet these macrocycles do not work alone. They stack together as a pair or trimer, which suggests a new way to enhance stability and direct structure with host-host contacts. However, such host-host interactions involving cyanostars are not strong enough to control co-assembly, as evidenced by the formation of mixtures^[14, 16] of products. To explore this novel idea fully for the first time, we employ a new class of macrocycle, the tricarbazole triazolophane,^[17] aka tricarb (**TC**, Figure 1b-d). This macrocycle has similar anion recognition to cyanostar but it displays stronger self-association^[17a] from favorable electrostatic interactions (dipole-dipole coupling) between π faces (Figure 1c and 1d). It is expected, therefore, that these host-host contacts stabilize architectures of discrete-numbers of stacked hosts.

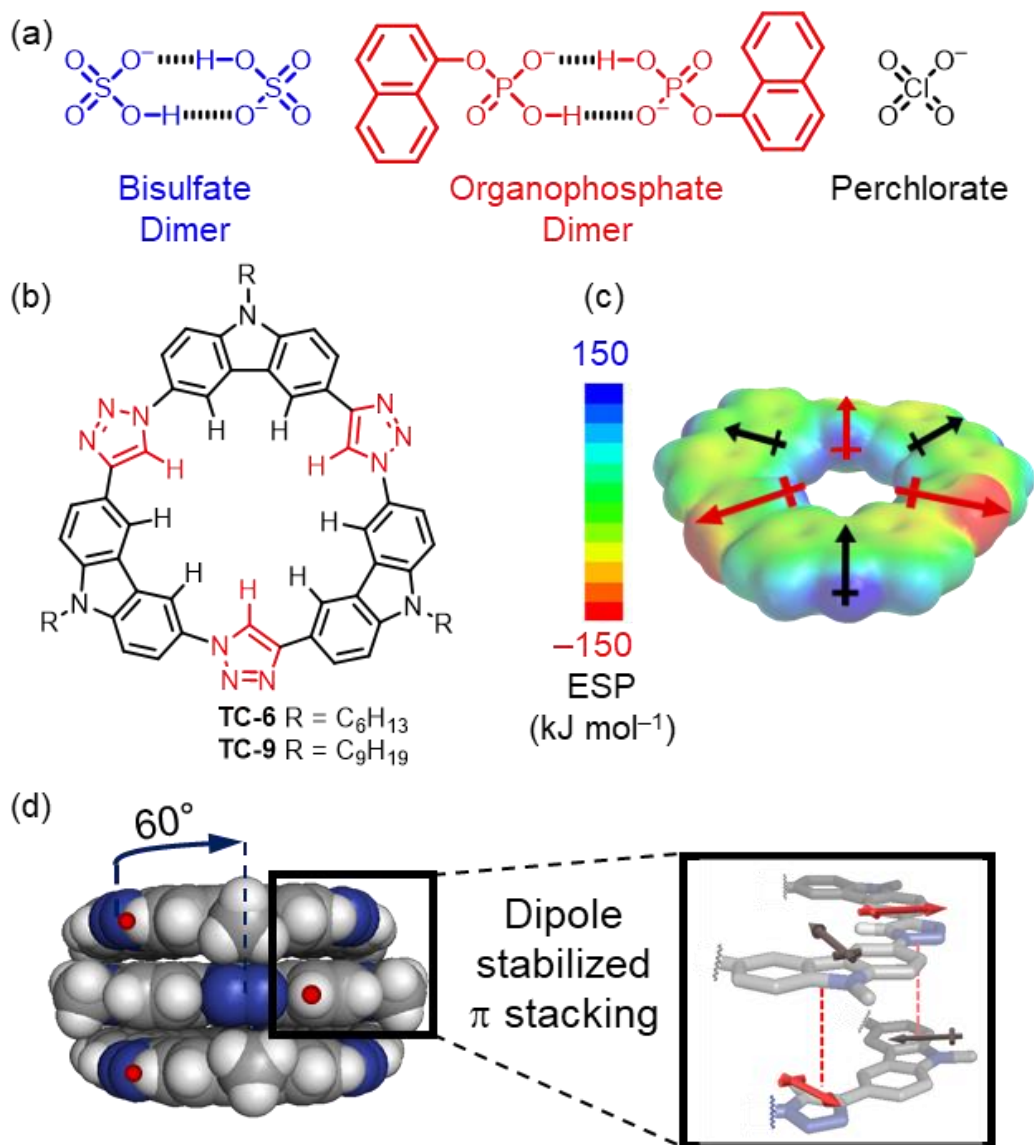
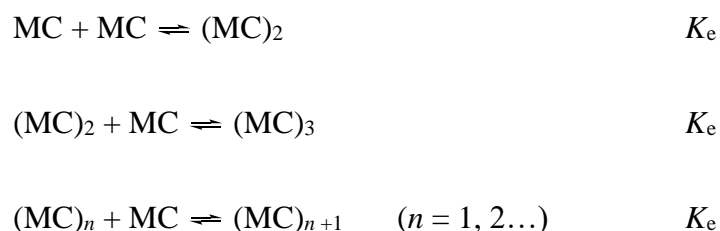


Figure 1. (a) Chemical structures of anionic guests employed in this study: bisulfate (HSO_4^-) dimer, naphthyl-phosphate (Np-HPO_4^-) dimer, and perchlorate (ClO_4^-). (b) Chemical structures of tricarb macrocycles **TC-6** and **TC-9**. (c) Electrostatic potential map of a single macrocycle. (d) Molecular model of the triple stack of tricarb macrocycles. Box shows complementary dipole interactions between triazole and carbazole units between π -stacked faces.

The role of host-host interactions in guest-directed self-assembly is poorly understood. Host-host interactions have been shown to play roles in determining the structure of self-assembled

building blocks,^[18] and the switching of the preferred chirality of helical structures.^[19] Insights into the role of hosts in anion-driven assembly are from indirect experiments.^[9c, 9e, 12a, 12b, 16b, 20] Host-host interactions can be characterized by their degree of self-association. For cyanostars, there is moderate self-association (Figure 2a) as evaluated using an isodesmic, equal- K model^[21] to be $K_e = 225 \text{ M}^{-1}$ (dichloromethane).^[14b] This equilibrium constant refers to the following reactions between macrocycles (MC):



When this host-host interaction was enhanced using solvent polarity, the mixture of bisulfate complexes shifted from favoring dimer stacks to trimers, i.e., from 2:2 to 3:2 macrocycle:anion complexes. The existence of host-host contacts was also hinted at by Kubik with his 2:2 tetra-pseudopeptide:phosphate complex.^[15e] In the solid state, the methyl groups of one receptor are observed to align with the aromatic rings of the second receptor. This observation led the authors to conclude that dispersion interactions between the two receptors may contribute to the overall stabilization of the complex. Further investigation of the host's self-association was not undertaken. Thus, it appears possible for host-host interactions to positively impact the complexes formed.

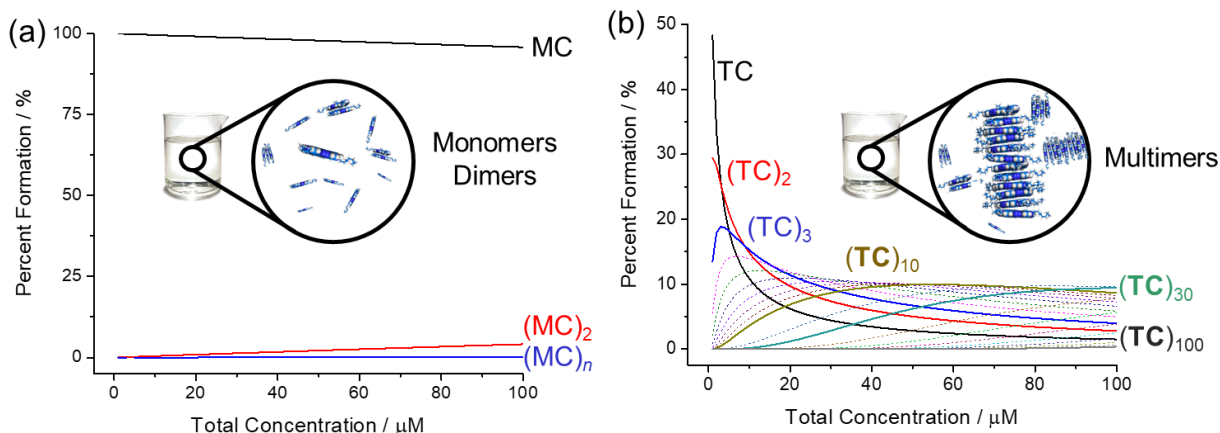


Figure 2. Distribution of hosts as higher-order multimers in the sub-0.1 mM concentration range predicted using the equal- K model for (a) cyanostar ($K_e = 225 \text{ M}^{-1}$) and (b) tricarb ($K_e = 800,000 \text{ M}^{-1}$).

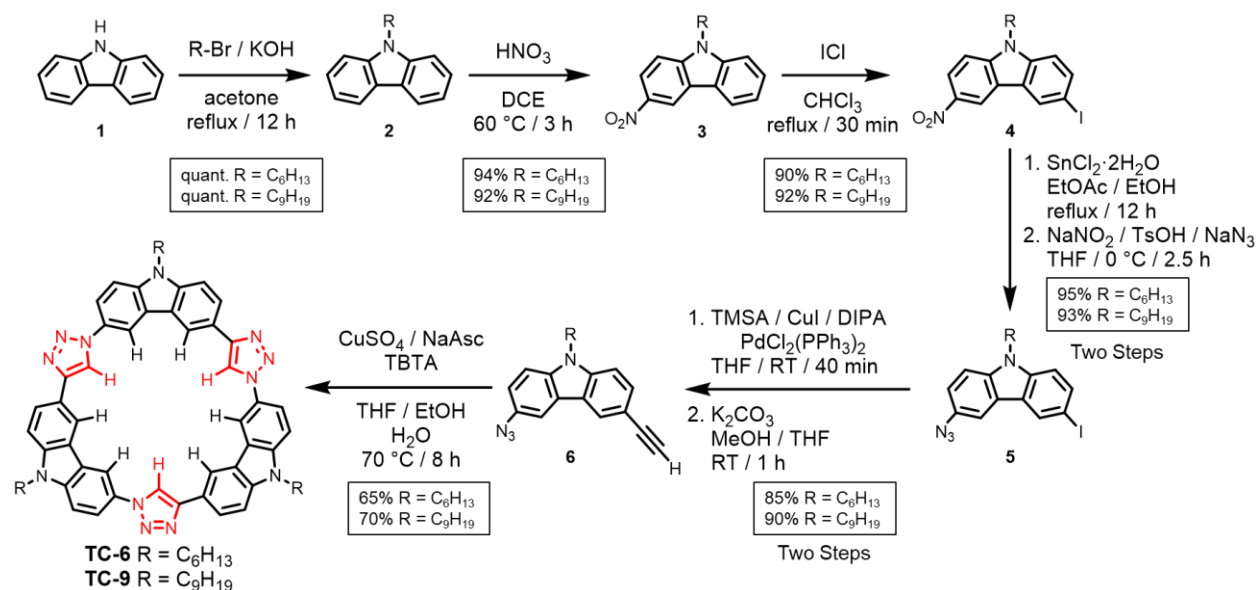
We provide the first investigation of the role of host-host interactions on the stability and hierarchical structure of hydroxyanion complexes. We take advantage of the tricarb macrocycle on account of its dominant, relative to other macrocycles,^[20b, 22] host-host self-association ($K_e \sim 10^5 \text{ M}^{-1}$),^[17a] which is three orders of magnitude larger than that of the cyanostar macrocycles ($K_e \sim 10^2 \text{ M}^{-1}$).^[14b] This situation produces a significant degree of multimer formation prior to addition of anions (Figure 2b); as expected, all behaviors contrast with the product mixtures seen with cyanostar. We prepared tricarb macrocycles with different alkyl chain lengths to both test the modularity of the synthesis^[17a] and to aid in structural characterization. Nonyl substituents (**TC-9**, $\text{R} = \text{C}_9\text{H}_{19}$, Figure 1b) provide solubility for performing binding studies while shorter hexyl chains enable crystal growth (**TC-6**, $\text{R} = \text{C}_6\text{H}_{13}$). Tricarb forms high-fidelity, triple decker stacks around bisulfate dimers in chloroform. Assignment as a 3:2 complex was supported by control studies using anions (Figure 1) that only form 2:2 (mononaphthyl phosphate, NpHPO_4^-) and 2:1 (perchlorate, ClO_4^-) complexes. Solvent conditions in which the macrocycle has lower self-

association shifted speciation to favor the 2:2 species further highlighting the importance of host-host interactions. This behavior enabled the realization of a solvent-driven switch between distinct triple and double-stacked architectures. The species and equilibria observed experimentally were also examined using density functional theory (DFT) and a continuum solvation model used previously with shape-persistent macrocycles.^[23] Computational results supported the solvent-responsive character resulting from host-host contacts. Furthermore, analysis of electrostatic potential maps showed that host-host contacts synergistically enhance the electropositive character of the binding pockets. These findings unambiguously verify the importance of host-host contacts in producing both discrete and responsive anion-templated architectures.

Results and Discussion

Macrocycle Synthesis

Tricarb macrocycles **TC-6** and **TC-9** were synthesized in a seven-step reaction sequence (Scheme 1) with good overall yields (45% and 50%, respectively), culminating in high yielding one-pot macrocyclizations. The route previously reported^[17a] was used with modest modification. Specifically, the conditions for the transformation of amino carbazole intermediate into azide **6** have been improved using milder conditions. Macrocyclizations for **TC-6** and **TC-9** from the corresponding difunctional precursors proceeded in 65% and 70% yields. Since our initial publication, Nakamura *et al.* have independently synthesized a similar macrocycle with dodecyl chains using different protocols.^[17b]



Scheme 1. Synthetic scheme for the one-pot syntheses of tricarbs **TC-6** and **TC-9** (1,2-dichloroethane, DCE; trimethylsilylacetylene, TMSA; diisopropylamine, DIPA; tris(benzyltriaazolymethyl)amine, TBTA).

Bisulfate Dimers Co-assemble with Triple-stacked Tricarb Macrocycles in Chloroform

All solution studies were undertaken with the soluble nonyl-substituted tricarb, **TC-9**. ^1H NMR titrations of the tricarb macrocycle (Figure 3a) with bisulfate show direct formation of the 3:2 species at 0.7 eq in chloroform. Early on in the titration we see the growth of a broadened set of aromatic proton resonances (black trace, Figure 3b) that convert into sharp peaks at 0.7 eq. All the inner protons (H^a , H^b , H^c) are shifted ~ 0.4 ppm downfield relative to the uncomplexed macrocycle, consistent with $\text{CH}\cdots\text{anion}$ binding.^[17a, 20c, 24] The bisulfate dimer resonance at 13.39 ppm, which is indicative of the formation of the dimer's self-complementary hydrogen bonds,^[14] shows maximal intensity at 0.7 eq. of added anion (Figure 3b). Intensity losses after this point are attributed to exchange with uncomplexed bisulfate anion. We also see that the aromatic signature

of the 3:2 complex persists even in the presence of a 25-fold molar excess of bisulfate. Such superstoichiometric conditions were seen previously with cyanostar to drive the formation of a 2:2:2 complex^[14b] at the expense of the 3:2 species in chloroform. These results show that the 3:2 bisulfate complex is both persistent and formed in high fidelity when using the self-associating tricarb macrocycle.

The signature for the 3:2 assembly is consistent with two outer and one inner macrocycle. The spectra show overlapping multiplets for protons H^d/H^g (~ 7.8 ppm, Figure 3c) and H^e/H^f (~7.2 ppm) assigned to the two different chemical environments of the outer (d, e, f, g) and inner macrocycles (d', e', f', g'). Additionally, the relative intensities of the aromatic protons (H^a–H^g, Figure S5) are consistent with previously observed tricarb macrocycle complexes.^[17a] Two-dimensional NMR (gCOSY, Figure S6) shows that four unique spin systems make up the observed multiplets. Exemplary of this assignment, correlations in the COSY NMR spectrum are observed between protons H^d at ~7.8 ppm and H^e at ~7.2 ppm (and H^g and H^f) on the outer macrocycles. This correlation is mirrored by protons H^{d'} and H^{e'} of the inner macrocycle. Consistently, no through-bond correlations exist between resonances assigned to protons of the inner and outer macrocycles.

Diffusion NMR experiments were undertaken to determine the size of the 3:2 complex by comparison to a 2:1 complex with perchlorate (ClO₄⁻). Consistently, the diffusion coefficient ($D_{2:1} = 3.11 \pm 0.04 \times 10^{-10} \text{ m}^2 \text{ s}^{-1}$) was larger than the 3:2 complex ($D_{3:2} = 2.89 \pm 0.03 \times 10^{-10} \text{ m}^2 \text{ s}^{-1}$). The volume ratios derived from the diffusion coefficients of the 3:2 and 2:1 complexes (1.07 ± 0.02 , Figure S16) match volume ratios derived from molecular models (1.12 ± 0.02).

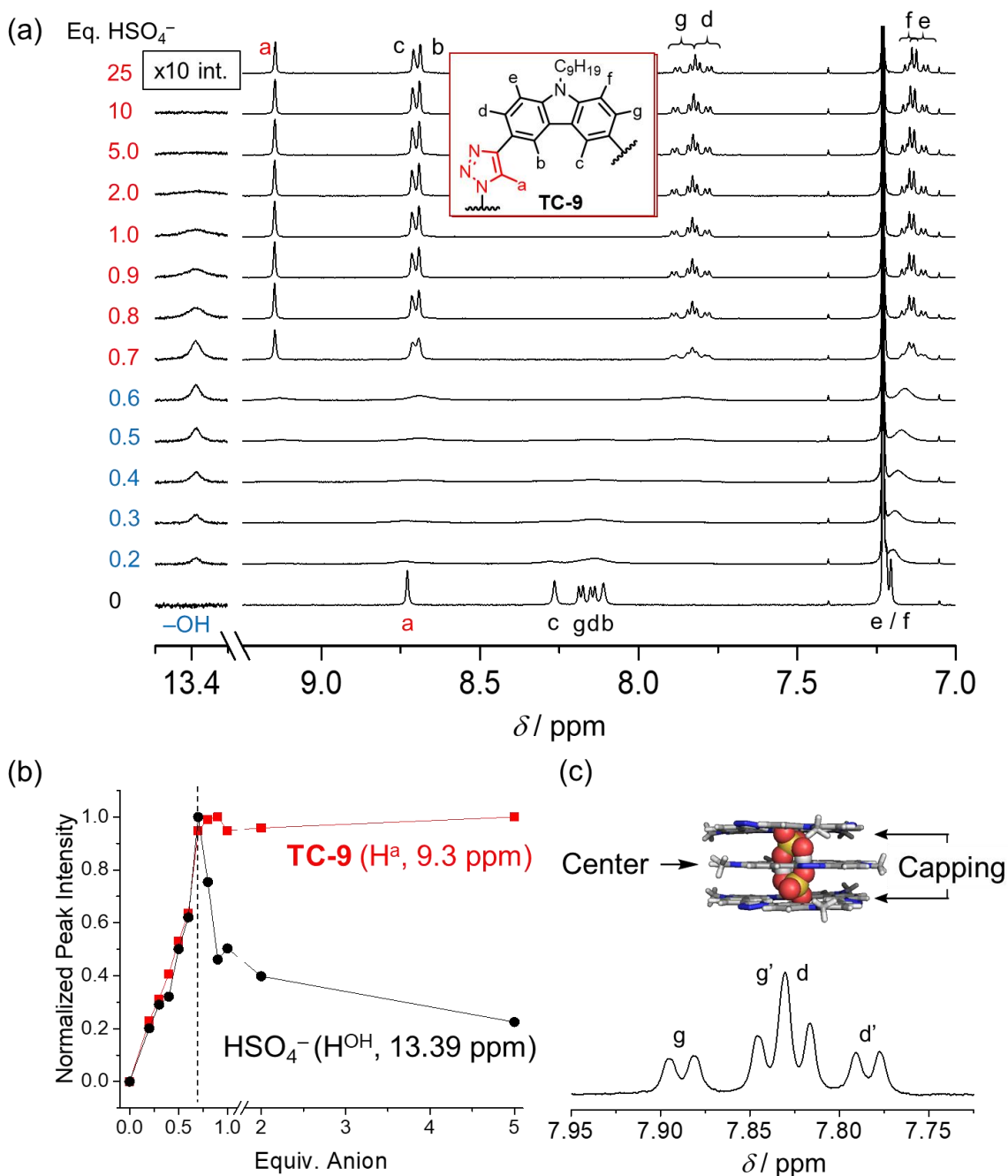


Figure 3. (a) ${}^1\text{H}$ NMR titration (600 MHz) of tricarb **TC-9** (1 mM) with HSO_4^- in CDCl_3 at 298 K. (b) Plot of normalized peak intensities of the triazole (H^a , red) and $[\text{HSO}_4 \cdots \text{HSO}_4]^{2-}$ dimer (H^{OH} , black) protons. Dashed line represents 0.7 eq. of HSO_4^- . (c) Expanded region of the ${}^1\text{H}$ NMR spectrum of the 3:2 assembly (1 mM, 0.7 eq. HSO_4^- , 298 K) showing the splitting of protons H^g , H^d , and $\text{H}^{d'}$.

The proton resonances and diffusion NMR of the tetrabutylammonium (NBu_4^+) cation were examined in order to gauge its possible involvement in ion pairing with the dianionic 3:2 complex in chloroform. The α -methylene protons of the NBu_4^+ cation remain stationary at 2.58 ppm from 0–0.7 equivalents of bisulfate indicating that ion pairing with the complex is either completely present (100%) or absent (0%). From 0.8–25 equivalents of added bisulfate, the α proton resonance shifts steadily downfield to 3.26 ppm consistent with the NBu_4^+ cation forming ion pairs with the excess bisulfate in solution. Diffusion NMR experiments (Figure S15) monitoring the tricarb's aromatic resonances at 0.67 eq. of added bisulfate confirm the absence of pairing between NBu_4^+ and the 3:2 complex. Consistently, the NBu_4^+ cation displayed a diffusion constant much larger than that for the 3:2 species ($D_{\text{NBu}_4^+} = 4.43 \pm 0.01$, $D_{\text{tricarb}} = 2.89 \pm 0.03 \times 10^{-10} \text{ m}^2 \text{ s}^{-1}$). These values lead to a large volume ratio of 3.55 ± 0.04 matching reasonably well with the volume ratio of ~ 4 obtained from space filling models of the species.

The high-fidelity and selective stabilization of the 3:2 species in chloroform is remarkable given the expectation of this low-dielectric solvent to serve as a strong medium for enlisting ion pairing to stabilize a 2:2:2 complex as was seen previously with cyanostar.^[14b] The preference of the 3:2 triple-decker tricarb complex over a 2:2:2 assembly was unexpected. For this reason, we speculated that the preference for the 3:2 may result from the steric exclusion of the cation from the dianion by the outer-most macrocycles. If this was the case, then the overall stability of the 3:2 complex would be expected to be poor. To assess the stability of the 3:2 complex, we conducted dilution experiments (5 mM to 5 μM , 0.7 eq. HSO_4^- , Figure S17). Surprisingly, the 3:2 complex persisted over all measured concentrations. This behavior is in striking contrast to the 2:2:2 cyanostar complex,^[14b] which instead dissociated into uncomplexed macrocycles below 50 μM .

The stability and selectivity for the 3:2 complex is attributed to strong host-host interactions. Consistently, speciation modelling^[25] of the self-association of tricarb alone (Figure S18) shows that stacks of three or more macrocycles dominate in solution at concentrations as low as 5 μM . Under the same conditions, cyanostar exists solely as a monomer. The differences in behavior between the two macrocycles reinforce the importance of host-host interactions in these co-assemblies.

Double-stacked Tricarb Complexes Form in More Polar Solutions

The substantial self-association of tricarb macrocycles is now believed to selectively stabilize the 3:2 complex in chloroform ($\epsilon = 4.8$) over all other possibilities. To further test this idea, NMR titrations were repeated in a solvent system of a higher polarity in a bid to weaken the intermolecular dipole-dipole contacts believed to enhance macrocycle self-association.^[17a]

A ^1H NMR titration of tricarb conducted in a more polar solution containing 20% v/v of added acetonitrile in chloroform ($\epsilon_{\text{mix}} \approx 12$, Figure 4)^[26] shows a signature for the 2:2 complex. With the addition of bisulfate, we see broadened peaks in the aromatic region settle into their final position and sharpen up at 1 eq. of anion. Additionally, aromatic protons H^{d} , H^{e} , H^{f} , and H^{g} do not split into the multiplet signature of the 3:2 assembly seen in neat chloroform confirming that a different complex is formed.

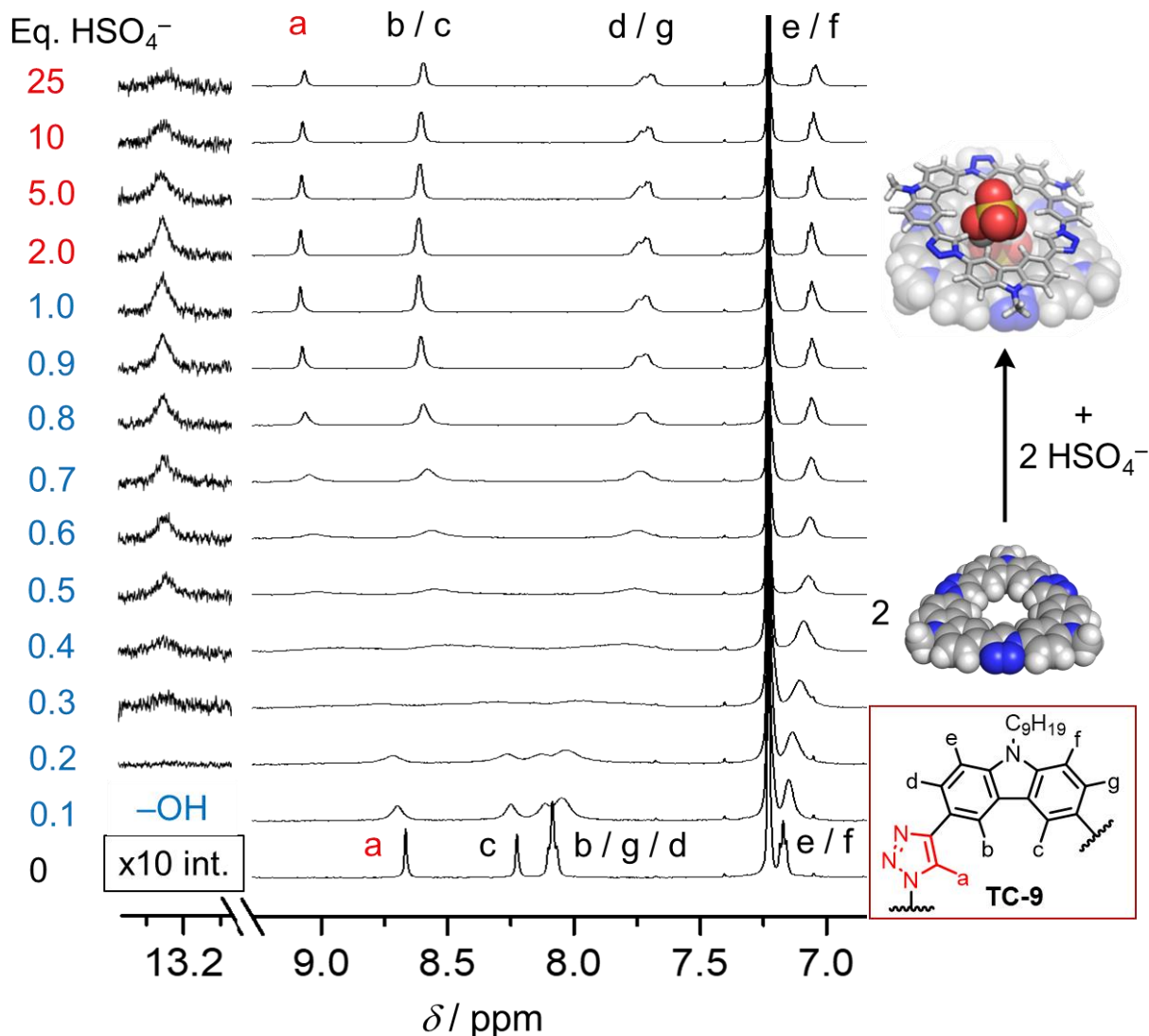


Figure 4. ^1H NMR titration (600 MHz) of tricarb **TC-9** (1 mM) with HSO_4^- in 20% v/v CD_3CN in CDCl_3 at 298 K in which a 2:2 complex is formed.

Upon cooling, the broad resonance assigned to the overlapping peaks of protons H^d and H^g resolves into two doublets (Figure 5). The observance of doublets is consistent with a 2:2 species in which the two macrocycles in the complex are in similar chemical environments. This outcome contrasts with the 3:2 complex where multiplets indicated two different environments for the inner and outer macrocycles.

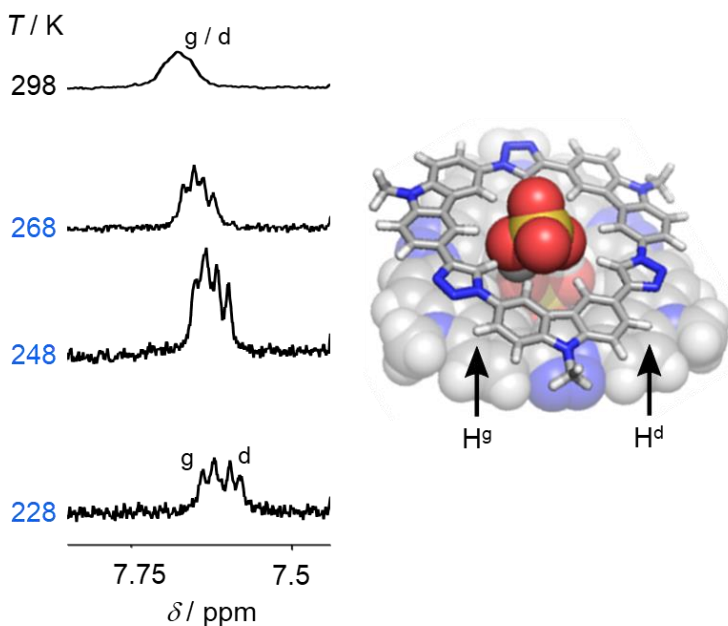


Figure 5. Variable temperature ^1H NMR spectra of protons H^{d} and H^{g} within the $[(\text{TC-9})_2(\text{HSO}_4)]^{2-}$ complex (1 mM, 1.0 eq. HSO_4^- , 20% v/v CD_3CN in CDCl_3 , 500 MHz).

The equivalence point of the titration of **TC-9** with bisulfate (1.0 eq.) and the variable temperature data strongly suggest the formation of a 2:2 species. The observation of a resonance for the bisulfate dimer at 13.2 ppm precludes the formation of a complex around a single anion (either a 2:1 or 1:1 species) in this mixed solvent system. Alternatively, the observed signature could also result from a 3:2 species that emerges a little later in the titration, coincidentally at 1 eq., as a consequence of weaker binding affinity (smaller β) in the polar solvent mixture. To distinguish between these two possibilities, we conducted titrations using a guest that is only capable of forming 2:2 species in order to establish its signature for comparison.

To definitively assign the complex formed between tricarb and bisulfate in polar solvents as the 2:2 species, we titrated tricarb with the mononaphthyl phosphate anion (NpHPO_4^- , Figure 6), which only forms a 2:2 complex on the basis of sterics.^[16a] The titration was conducted in 20%

v/v acetonitrile in chloroform. The chemical shifts of the 2:2 product are consistent with the titrations seen with bisulfate, including the overlapping of protons $H^{d/g}$ and $H^{e/f}$. The peak shifts for the 2:2 complex observed upon the addition of mononaphthyl phosphate to tricarb show the internal protons of the macrocycle (H^a , H^b , H^c) are shifted further downfield than is observed with bisulfate, consistent with behavior seen with cyanostar.^[14b, 16a] Plots of normalized titration data (Figure 6c) reveal that the 2:2 $NpHPO_4^-$ complex (blue) and the assembly formed between tricarb and HSO_4^- (red) in the acetonitrile mixture follow identical titration curves. The similarities between the titrations of tricarb macrocycles with the HSO_4^- and $NpHPO_4^-$ anions support the assignment of a 2:2 bisulfate complex in the 20% v/v solvent mixture.

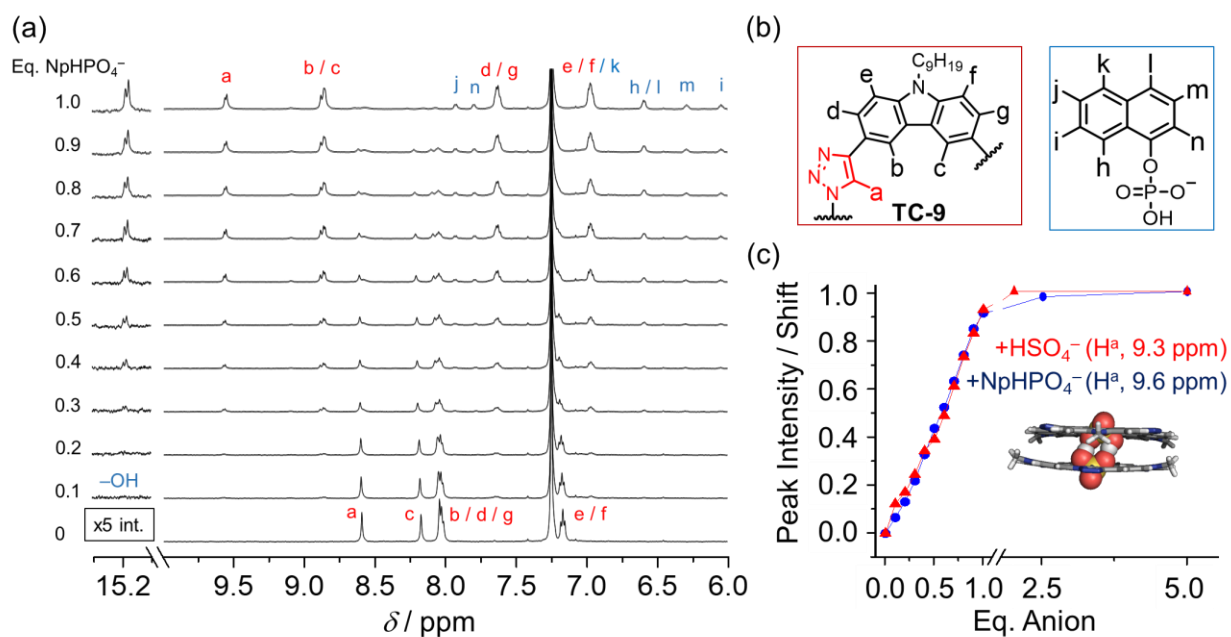


Figure 6. (a) 1H NMR (600 MHz) titration of tricarb **TC-9** (1 mM) with $NpHPO_4^-$ in 20% v/v CD_3CN in $CDCl_3$ at 298 K. (b) Chemical Structure and peak labels of tricarb (red) and $NpHPO_4^-$ (blue). (c) Plot of the normalized peak shift of proton H^a upon the addition of HSO_4^- (red) and normalized peak intensity of proton H^a upon the addition of $NpHPO_4^-$ (blue) in 20% v/v CD_3CN in $CDCl_3$ at 298 K.

The ^1H NMR spectrum of the 2:2 tricarb complex with $[\text{NpHPO}_4\cdots\text{NpHPO}_4]^{2-}$ displays resonances at ~ 15.2 ppm for the self-complementary *anti*-electrostatic hydrogen bonded phosphate homodimer. Through-space correlations are observed in the ^1H - ^1H ROESY NMR experiments on the 2:2 complex when conducted in chloroform (Figure S9). These correlations indicate a close spatial relationship between protons of the self-complementary hydrogen bond of the phosphate dimer and the inner CH hydrogen bonding protons of the tricarb macrocycles (H^a , H^b , H^c). Thus, these correlations place the homodimer inside the macrocyclic cavities.

The pairs of closely-spaced peaks in the ^1H NMR signature of the 2:2 complex with naphthyl phosphate indicate the presence of diastereomers. The parent tricarb macrocycles are prochiral and when viewed from one face the macrocycles can be distinguished stereochemically by their clockwise (*P*) and counter-clockwise (*M*) priority directions.^[17a] When the macrocycles undergo anion binding to form the 2:2 complex, their plane of symmetry is lost. Thus, *meso* (*MP* combinations of π -stacked macrocycle dimers) and *chiral* (*MM* and *PP*) diastereomers of dimer stacks are possible and are observed in the spectrum of the 2:2 complex.

Two phosphate dimer peaks (15.19 and 15.21 ppm) reflect diastereomeric pairs of the **TC-9** macrocycles in the 2:2 complex. We assign these peaks to a pair of diastereomers rather than ^{31}P - ^1H coupling on account of the fact that both the peak-to-peak separation (15 Hz) and sharpness of the peaks are inconsistent with typical $^2\text{J}_{\text{PH}}$ coupling of 20-30 Hz.^[27] Diastereomers are also seen with protons H^a , H^b , and H^c . The observation of diastereomeric peaks has been seen previously in 2:2 complexes of hydroxyanions with cyanostar.^[14b, 16, 28] Within such complexes the position of one cyanostar macrocycle relative to the other was fixed in place as a result of the steric gearing between the macrocycle's bulky substituents. The fixed positions allow the unique chemical environments in the *meso* (*MP*) and *chiral* (*MM* and *PP*) diastereomers to be

resolved.^[24d] First, the fact that we see unique chemical resonances in the naphthyl phosphate complex indicates that the diastereomers are in slow exchange with each other. Second, we also posit that resolution of unique chemical shifts for the diastereomers reflect a relatively fixed rotation angle between π -stacked tricarb macrocycles. While these macrocycles do not have the steric gearing seen with cyanostar, the complementary host-host interactions between tricarb macrocycles (dipole-enhanced π -contacts, Figure 1d) might serve a similar purpose. Without fixed rotational configurations, we would expect dynamic rotational effects to lower differences between the resonant frequencies of diastereotopic protons in the *meso* and *chiral* combinations of macrocycles.

Solvent-driven Switching

The solvent-dependent preferences of bisulfate complexes were used as a basis for developing an environmentally responsive switch between the triple and double stacked species (Figure 7). To a solution of the 3:2 complex present (5 mM, 1 eq. HSO_4^-) in chloroform ($\epsilon = 4.8$) was added 20% *v/v* acetonitrile ($\epsilon_{\text{mix}} \approx 12$). Upon the increase in solvent polarity, the 3:2 complex was observed to fully convert to the 2:2 species as confirmed by ^1H NMR spectroscopy. To determine if the 2:2 species could be converted back to the 3:2 complex, the polarity of the 2:2 solution was lowered by the addition of carbon tetrachloride ($\epsilon = 2.24$). Upon decreasing the dielectric constant of the solvent mixture to that resembling pure chloroform ($\epsilon_{\text{mix}} \approx 5$), we were able to observe the restoration of the ^1H NMR spectrum for the 3:2 species. The ability to switch between species solely by changing solvent composition demonstrate the solvent-responsive, host-host interactions in the bisulfate complexes with tricarb.

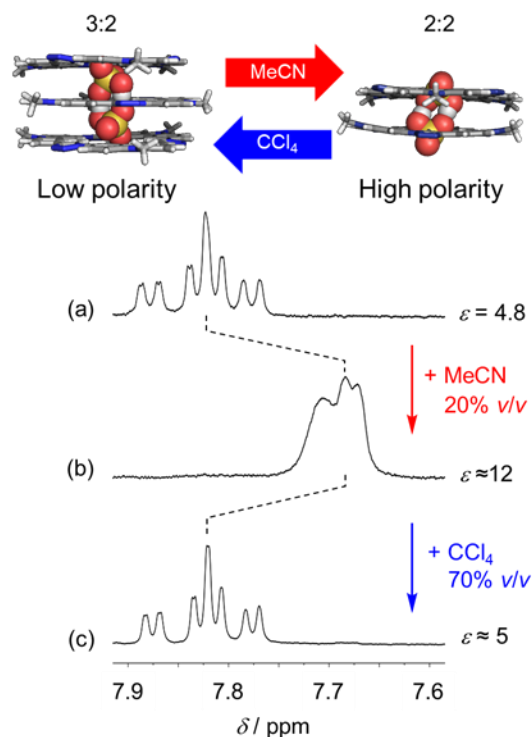


Figure 7. Solvent driven switching demonstrated using ^1H NMR spectra (protons H^{d} and H^{e}) of (a) the 3:2 tricarb:bisulfate complex (5 mM **TC-9**, 1.0 eq. HSO_4^-) in chloroform, (b) the 2:2 complex after the addition of acetonitrile to form a 20% v/v mixture, and (c) the restored 3:2 complex following the addition of carbon tetrachloride (500 MHz, 298 K).

Crystal Structure

We were able to characterize the bisulfate complex by crystallography in what also serves as the first crystal structure of tricarb macrocycles (Figure 8). Crystals were grown by vapor diffusion of diethyl ether ($\epsilon = 4.3$) into a chloroform solution ($\epsilon = 4.8$) containing tricarb **TC-6** and 1 eq. of NBu_4HSO_4 . X-ray crystallography shows the hydrogen-bonded bisulfate dimer is encapsulated inside two tricarb macrocycles all bookended by a pair of NBu_4^+ cations to give a complex of 2:2:2 overall stoichiometry. The bisulfate dimer contains a pair of $\text{OH}\cdots\text{O}$ hydrogen

bonds with oxygen-oxygen distances of $d_{\text{OO}} = 2.61 \text{ \AA}$, consistent with moderate hydrogen-bonding^[29] and within the range of other bisulfate dimers observed in the solid state.^[14a] It is now accepted^[11d, 30] that these short-range hydrogen bonds help to partially offset the long range Coulombic repulsions between the anionic charges. Further stabilization comes from the two tricarb macrocycles contributing 18 C–H hydrogen bonds to the doubly charged anion dimer ranging in length from 2.34 to 3.04 \AA $d_{\text{CH}\cdots\text{O}}$. In addition, the two ends of the bisulfate dimer protrude from the binding pocket. These exposed ends form four close CH \cdots O hydrogen bond contacts ($d = 2.39\text{--}3.08 \text{ \AA}$) and offer proximal ion pairing with the two NBu_4^+ cations helping to further stabilize the dimer species. These structural characteristics closely match the 2:2:2 structure seen with cyanostar.^[14a] This similarity allows us, therefore, to attribute differences in behavior between the two macrocycles to host-host interactions.

This crystal structure shows that the ion-paired 2:2:2 structure is favored upon crystallization despite the 3:2 species' stability in the low-polarity solvents of crystallization. Presumably a π -stacked tricarb dimer (**TC-6**)₂ enables greater ionic stabilization energy to be gained from the two NBu_4^+ cations and the dianionic dimer ($\text{HSO}_4\cdots\text{HSO}_4$)²⁻ and thus higher lattice energy per unit volume than would be possible with a triple stack of macrocycles (**TC-6**)₃. This argument is reasonable when considering that a triple stack of tricarb macrocycles will spatially isolate the bisulfate dimer from the cations. Longer distances lower Coulombic stabilization and also exclude formation of cation-to-anion CH \cdots O hydrogen bonds. Presumably, these factors tip the balance in favor of the 2:2:2 in the solid state.

Gratifyingly, the crystal structure also verifies the hierarchical 2D and 3D packing of tricarb macrocycles postulated^[17a] from the interpretation of scanning tunneling microscopy (STM) imaging and solution-phase studies of self-association. The two π -stacked macrocycles

have a very short inter-planar distance of 3.37 Å and they are rotated 58° with respect to one another. This rotational angle was originally correlated with the macrocycle's substantial self-association.^[17a] This angle maximizes the favorable local-dipole interactions between macrocycles and supports the idea that the large host-host interactions are best characterized as dipole-stabilized π -stacking.^[20b]

Another feature observed in the solid state are the lateral inter-macrocycle contacts that extend packing in two dimensions (Figure 8c-f). These contacts form a donor-acceptor (D-A) seam of hydrogen bonding matching a quadruple DDAA array.^[31] At this lateral seam, we see the triazoles of one macrocycle are oriented in the same way as the triazoles of its neighboring macrocycle. That is, with the bridgehead nitrogens of the 1,2,3-triazoles at the center of the DDAA array. By extension, neighboring macrocycles all have the same handedness; clockwise is shown in Figure 8d. The other possible arrangement is for neighboring macrocycles to have opposite chiralities: clockwise-counterclockwise. This mixed arrangement is not observed in the solid state. As elaborated elsewhere,^[17a] the preferred lateral combination (Figure 8f) was identified previously with the aid of calculations (B3LYP/6-31G*) using a dimer composed of smaller, model fragments. We attributed this preferred arrangement to more favorable dipole-dipole pairing (Figure 8f) of the large 5-Debye molecular dipoles on the triazole moieties within the lateral plane of the macrocycles.

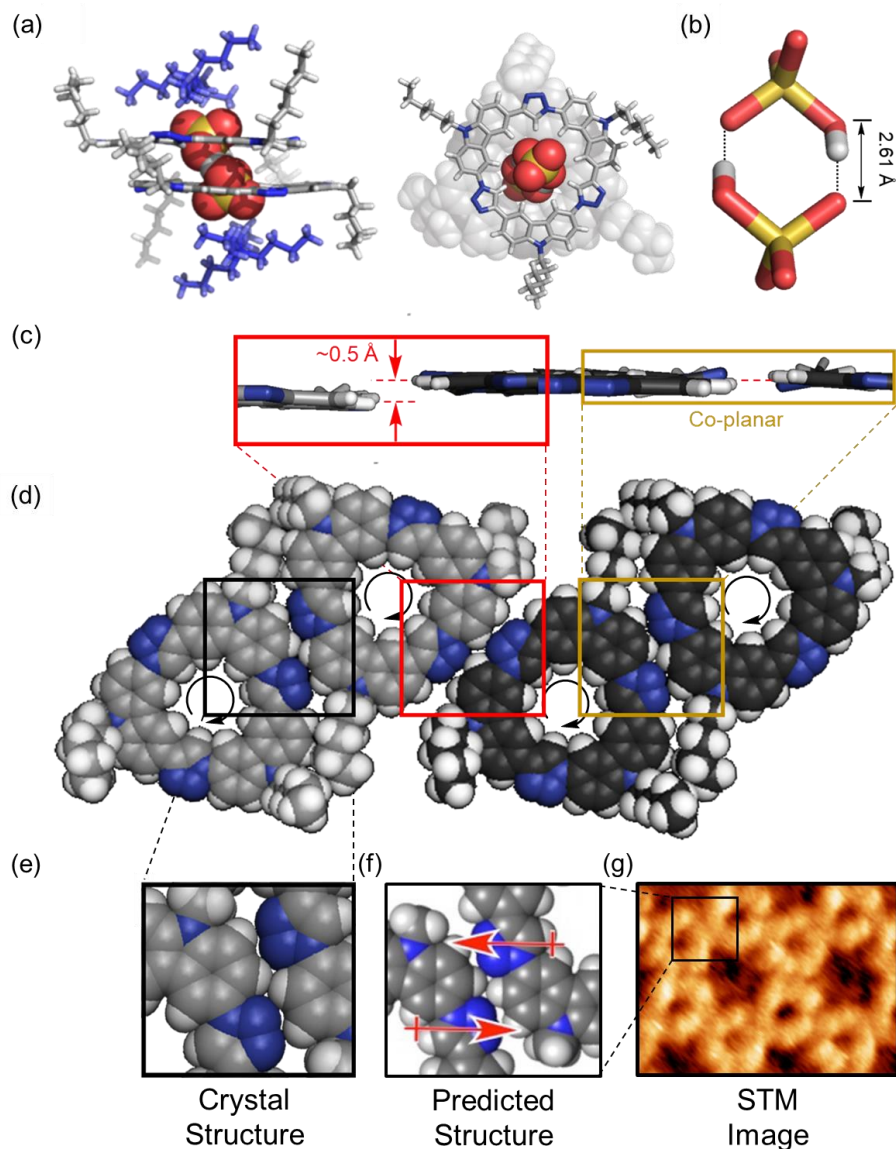


Figure 8. (a) Crystal structure showing the 2:2:2 (TC-6)₂(HSO₄)₂(NBu₄)₂ complex from the side and top-down. NBu₄⁺ cations have been removed from the top-down view for clarity. (b) Side view of the encapsulated [HSO₄•••HSO₄]²⁻ dimer. (c) Side view showing how each tricarb macrocycle has one in-plane and one out-of-plane seam. (d) Top view showing orientations of neighboring macrocycles as pairs (left pair with grey carbons; right pair with black carbons). (e) The lateral contacts between tricarb macrocycles within the crystal structure, (f) the predicted

orientation of the lateral seam of tricarb macrocycles based on DFT (B3LYP, 6-31G*) calculations of lateral homodimerization energies and (g) STM imaging of the lateral seam.

Computations and Virtual Experiments

The totality of the experimental data indicates that host-host interactions can play a deciding role in selecting the complexes seen in solution. To probe this idea further, we conducted DFT calculations on the key tricarb species (free macrocycle, macrocycle dimer, macrocycle trimer, HSO₄⁻, HSO₄⁻ dimer, 1:1, 2:1, 1:2, 2:2, 2:2:2, and 3:2 complexes). A model of the tricarb macrocycle (**TC***) was used in all calculations in which the alkyl chains were truncated to hydrogen atoms. Similarly, the tetrabutyl ammonium (NBu₄⁺) cation was replaced with tetramethyl ammonium (NMe₄⁺). The initial geometry of the 2:2:2 assembly was taken from the crystal structure and then fully optimized. The model for the triple stack was generated from the placement of the third macrocycle into π - π contact and rotated 60° atop the original 2:2 complex to extend the packing seen in the solid state and then followed by geometry optimization. All other geometries were independently optimized at the B97D3/6-31+G(d) level in the gas phase.

The geometry of the bisulfate dimer within the truncated model of the 2:2:2 complex, [(**TC***)₂(HSO₄•••HSO₄)(TMA)₂], is in good agreement with the observed solid-state structure (see Supporting Information, Figure S24). In particular, the oxygen-oxygen distance (d_{oo}) in the bisulfate dimer was calculated to be 2.67 Å compared to a 2.61 Å in the solid state. The interplanar distance between tricarb macrocycles in the calculated structure (3.29 Å) is in excellent agreement with the crystal structure (3.37 Å).

The good correspondence between calculation and experiment provided a basis to evaluate the overall stability of the various complexes in solution. Here, we calculated energies of the various species (1:1, 2:1, 2:2, 3:2, 2:2:2) in solution using ONIOM(MP2/6-311++G(d,p):B97D3/6-311++G(d,p) with implicit solvation (IEF-PCM model). The solvation energies also showed a good correspondence to prior work on triazolophanes.^[23] Specifically, the solvation free energy of tricarb in chloroform ($-19 \text{ kcal mol}^{-1}$) closely matches the value for an analogous, albeit slightly smaller, triazolophane ($-14.7 \text{ kcal mol}^{-1}$). Calculations on the latter^[23] were able to successfully reproduce experimental free energies for chloride binding as a 1:1 complex and, thus, serve as an indication of the accuracy of the solvation model and energies in both cases.

Free energy calculations of all the relevant species corroborate our observations from experiment (see Supporting Information, Table S2). The calculations show that the bisulfate dimer, $[\text{HSO}_4 \cdots \text{HSO}_4]^{2-}$, is not stable in chloroform ($+30 \text{ kJ mol}^{-1}$) relative to two individually solvated anions. This is consistent with variable concentration studies performed elsewhere^[14b] that show the bisulfate anion does not dimerize alone in solution, at least up to 1 M.

The 3:2 complex is the only species observed experimentally in chloroform. We probed this idea computationally by using a balanced reaction that interconverts between the 2:2 and 3:2 species at the 0.67 equivalence point:



The free energy for this equilibrium (Eq. 1) was calculated to be $\Delta G = -134 \text{ kJ mol}^{-1}$, verifying preferential formation of the 3:2 species over the 2:2. When the same equation is modified to

consider inclusion of ion pairing to help enhance the 2:2:2 assembly, the balanced reaction still favors the 3:2 species.

When the recognition chemistry was studied experimentally in the mixed solvent containing 20% *v/v* acetonitrile in chloroform, the balance is tipped to favor the 2:2 complex. At 1.0 eq. of bisulfate, these conditions are represented by the following balanced equation:



The calculated free energy for this reaction ($\Delta G = +83 \text{ kJ mol}^{-1}$) favors the left-hand side of the reaction and is again consistent with our observation.

The fact that the computed reaction free energies match qualitatively with experimental observations provides a basis to consider the possible underlying driving forces. The first is the dipole-enhanced π -stacking, which is found experimentally to be more favored in solvents of lower dielectric as a result of strengthened intermolecular contacts. To this end, the free energy of dimerization was calculated using the following equation:



Consistently, dimerization of the tricarb macrocycle, **TC***, was calculated to be 10 kJ mol^{-1} more favorable in pure chloroform than in the 20% *v/v* acetonitrile in chloroform solvent mixture (see Supporting Information, Table S4).

The computed 1:1 and 2:1 anion binding energies can be compared to experimental values. Previous studies on cyanostar-anion complexes show absolute binding energies of the 1:1 complexes with perchlorate from theory (-42 kJ mol^{-1}) and experiment ($< -20 \text{ kJ mol}^{-1}$) are on similar orders of magnitude.^[14a] That similarity was seen to be lost for the double-stacked

cyanostar complexes, as the calculated energy of the 2:1 complex of perchlorate (-163 kJ mol^{-1})^[14a] is overestimated substantially (by 95 kJ mol^{-1}) compared to the experimentally derived value. Similar overestimations are also likely to be present for the calculated energies of the dimer and trimer complexes of tricarb as both sets of complexes have similar computed stabilities. We are currently performing a series of systematic investigations to calibrate the interactions energies of systems with large π surfaces to understand the factors that control stacking energies in such molecules; most prior works^[32] have only examined small π -systems. However, this overestimation associated with stacking interactions is expected to be systematic across similar species, and we expect that the trends derived from the signs of the free energy changes for the reactions considered above to be reliable. Thus, our computational model lends support to the essential conclusions of this paper.

Finally, we investigated the idea that stacking of macrocycles enhances the electrostatic cavity. To this end, we calculated the electrostatic potential maps (ESP, B3LYP-D3 6-31G*, Figure 9) for the monomer, dimer, and trimer stacks of tricarb macrocycles. Average ESP values were determined from the ESP of each hydrogen atom within the binding cavity. The monomer displays an average ESP of 139 kJ mol^{-1} . Upon dimerization the average ESP of each macrocycle increases 10% to 154 and 156 kJ mol^{-1} . The insertion of a third macrocycle in the trimer produces average ESP values for the outer macrocycles that dropped a little to 149 and 151 kJ mol^{-1} . However, the central macrocycle's average ESP grows again to 161 kJ mol^{-1} . Interestingly, while the total average ESP value for the trimer (154 kJ mol^{-1}) is 15 kJ mol^{-1} larger than the monomer, it is 1 kJ mol^{-1} smaller than for the dimer. Overall, stacking enhances the electropositive character of the binding cavity of tricarb macrocycles with the greatest benefit offered upon dimerization.

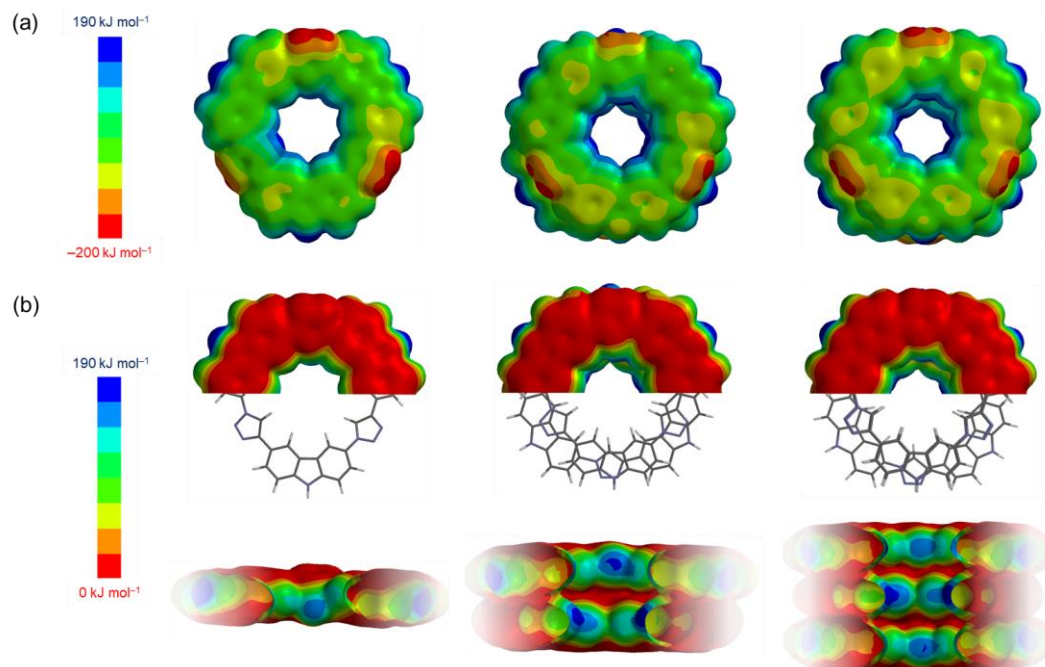


Figure 9. (a) Electrostatic potential (ESP, B3LYP-D3 6-31G*) maps of the tricarb model (TC*) as a monomer TC*, dimer (TC*)₂, and trimer (TC*)₃. (b) Top-down and side on views of rescaled ESP maps showing the interior of the macrocycles.

Conclusions

We have clearly demonstrated that host-host interactions can play a significant role in the structure and stability of anion-directed assemblies. We showed that the strong self-association of tricarb macrocycle hosts drives the formation of triple-stacked 3:2 complexes with bisulfate dimers in high fidelity. Weakening of the dipole-stabilized π -stacking between macrocycles by modulating the solvent environment resulted in complexes composed of just two stacked macrocycles. This solvent sensitivity provided a means to create solvent-driven switching between the triply and doubly stacked complexes. The crystal structure verified the strong dipole-stabilized π -stacking from the structural characteristics. Computational studies corroborated the solvent

dependent preferences underscoring, again, the importance of host-host interactions. Electrostatic potential maps show that host-host interactions can also synergistically enhance the electropositive binding cavity. This work deepens our knowledge of how macrocyclic self-association influences the structures and stabilities of discrete and responsive architectures co-assembled with hydroxyanions and it constitutes a new basis for multicomponent hierarchical assembly.

Experimental Section

General Methods for Synthesis

All reagents were obtained from commercial suppliers and used as received unless otherwise noted. The tetrabutylammonium salts NBu_4HSO_4 (Sigma Aldrich) and NBu_4ClO_4 (TCI America) were used as received and stored under argon. The tetrabutylammonium salt $\text{NBu}_4\text{NpHPO}_4$ was prepared according to a previously reported procedure^[16a] and stored under argon. Deuterated solvents CDCl_3 (Sigma Aldrich) and CD_3CN (Cambridge Isotope Laboratories) were used as received. Column chromatography was performed on silica gel (160-200 mesh, Sorbent Technologies, USA). Thin-layer chromatography (TLC) was performed on pre-coated silica gel plates (0.25 mm thick, #1615126, Sorbent Technologies, USA) and observed under UV light. Nuclear magnetic resonance (NMR) spectra were recorded on Varian Inova (600 MHz, 500MHz, and 400 MHz) and Varian VXR (400 MHz) spectrometers at room temperature (298 K) unless otherwise indicated. Chemical shift positions were determined using solvent residue peaks. IR spectra were recorded using a PerkinElmer Spectrum Two FT-IR as Nujol mulls on NaCl salt plates. High-resolution mass spectroscopy (HRMS) utilizing electrospray ionization (ESI) and

electron ionization (EI) was performed on a Thermo Electron Corporation MAT 95XP-Trap mass spectrometer.

General Methods for ^1H NMR Titrations

Titrations were monitored by ^1H NMR spectroscopy. In a typical ^1H NMR titration, 0.5 mL of a **TC-9** (1 mm) solution was prepared in a screw-cap NMR tube equipped with a PTFE/silicone septum. The salt solutions (50 mM) were prepared immediately before use and stored in screw-cap vials equipped with PTFE/silicone septa. Salt solutions were added using Hamilton gas-tight syringes (10, 50, 500 μL).

General Methods for Calculations

All computations were carried out using the Gaussian (G16) program suite. Models of the tricarb macrocycle (**TC***) in which the alkyl chains were replaced with terminal hydrogen atoms were used for all calculations. All calculated species were fully geometry optimized in the gas phase using B97D3/6-31+G(d). The B97D3 functional was chosen for its ability to capture the π -stacking interactions accurately, as recommended by Sherrill^[32a, 32b] and Wheeler.^[33] Frequency calculations were performed using B97D3/6-31+G(d). All calculated geometries were confirmed to be minima with no imaginary frequencies. As the low-lying vibrational frequencies are known to be inexact in the rigid-rotor harmonic approximation, herein the vibrational entropy for all the modes with frequencies $< 200\text{ cm}^{-1}$ have been replaced by corresponding free-rotor entropy. Single point energy calculations were carried out using two-layer ONIOM(MP2/6-311++G(d,p):B97D3/6-311++G(d,p)) in the gas-phase. Solution-phase (chloroform, 20% v/v acetonitrile/chloroform solvent mixture) calculations were carried out using an integral equation formalism polarizable continuum (IEFPCM) model. Electrostatic potential map calculations were

carried out using DFT methods at the B3LYP-D3 level with the 6-31G* basis set. First, points were found to define a surface with an electron density of 0.002 a.u. Second, the electrostatic potential was generated by rolling an imaginary positive charge over this iso density surface.

Synthesis and Characterization

9-Hexylcarbazole (C₆-2) – A mixture of carbazole (1 g, 6 mmol), 1-bromohexane (1.01 mL, 7.2 mmol), and KOH (0.5 g, 9 mmol) in acetone (100 mL) was heated to reflux overnight. After removing the solvent in vacuo, the mixture was extracted with EtOAc and washed with water. Column chromatography on silica gel using hexanes resulted in a clear oil (1.47 g, 5.9 mmol, quant. yield). The ¹H NMR spectrum was identical to previous reports.^[34]

9-Nonylcarbazole (C₉-2) – Compound **C₉-2** was prepared as a colorless oil following the same procedure as **C₆-2** in quant. yield from carbazole and 1-bromononane. The ¹H NMR spectrum was identical to previous reports.^[35]

9-Hexyl-3-nitrocarbazole (C₆-3) – A solution of **C₆-2** (1.47 g, 5.9 mmol) in 1,2-dichloroethane (50 mL) was cooled to 0°C (ice bath), to which nitric acid was added dropwise (16 M, 0.4 mL, 6.6 mmol). The reaction was heated to 60 °C and stirred for 3 h. After cooling to room temperature, water was added, and the mixture was extracted with CH₂Cl₂. The organic layer was dried with MgSO₄, filtered, and the solvent was removed in vacuo. The crude solid mixture was recrystallized from hexanes to give an orange solid product (1.64 g, 5.55 mmol, 94% yield). The ¹H NMR spectrum was identical to previous reports.^[34]

9-Nonyl-3-nitrocarbazole (C₉-3) – Nitro **C₉-3** was prepared as an orange solid following the same procedure as **C₆-3** in 92% yield from **C₉-2**. ¹H NMR (400 MHz, chloroform-*d*) δ / ppm = 8.98 (d, J = 2.2 Hz, 1H), 8.35 (dd, J = 9.1, 2.2 Hz, 1H), 8.12 (d, J = 7.8 Hz, 1H), 7.53 (t, J = 7.7 Hz, 1H),

7.44 (d, $J = 8.2$ Hz, 1H), 7.37 (d, $J = 9.1$ Hz, 1H), 7.32 (t, $J = 7.5$ Hz, 1H), 4.31 (t, $J = 7.3$ Hz, 2H), 1.93 – 1.78 (m, 2H), 1.51 – 1.06 (m, 12H), 0.83 (t, $J = 6.8$ Hz, 3H). ^{13}C NMR (100 MHz, chloroform-*d*) δ / ppm = 143.48, 141.57, 140.50, 127.30, 122.79, 122.49, 121.56, 120.94, 120.67, 117.30, 109.64, 108.20, 43.58, 31.74, 29.37, 29.28, 29.14, 28.86, 27.19, 22.57, 14.03. HRMS (EI) calculated for $\text{C}_{21}\text{H}_{26}\text{N}_2\text{O}_2 + \text{H}$: 339.1994 $[\text{M}+\text{H}]^+$; found: 339.2070.

9-Hexyl-3-iodo-6-nitrocarbazole (C₆-4) – To a solution of **C₆-3** (1.64 g, 5.6 mmol) in CHCl_3 (75 mL) was added ICl (1 g, 6.2 mmol), and the mixture was stirred at room temperature for 1 h, then heated at reflux for 30 min. The reaction progress was checked by ^1H NMR spectroscopy. The reaction was quenched by adding an aqueous solution of sodium bisulfite and stirred for 20 min. The mixture was extracted with CH_2Cl_2 , dried with MgSO_4 , filtered, and then concentrated in vacuo. The crude product was hot-filtered from hexanes to give a yellow solid (2.13 g, 5.04 mmol, 90% yield). ^1H NMR (400 MHz, chloroform-*d*) δ / ppm = 8.93 (d, $J = 2.2$ Hz, 1H), 8.44 (d, $J = 1.6$ Hz, 1H), 8.37 (dd, $J = 9.1, 2.2$ Hz, 1H), 7.78 (dd, $J = 8.6, 1.6$ Hz, 1H), 7.38 (d, $J = 9.2$ Hz, 1H), 7.32 – 7.04 (m, 2H), 4.29 (t, $J = 7.2$ Hz, 2H), 1.84 (p, $J = 7.2$ Hz, 2H), 1.38 – 1.17 (m, 6H), 0.83 (t, $J = 6.7$ Hz, 3H). ^{13}C NMR (100 MHz, chloroform-*d*) δ / ppm = 143.29, 140.75, 135.61, 129.81, 127.31, 125.13, 122.11, 121.17, 117.45, 111.60, 108.50, 83.31, 43.70, 31.42, 28.81, 26.83, 22.46, 13.94. HRMS (EI) calculated for $\text{C}_{18}\text{H}_{19}\text{IN}_2\text{O}_2$: 422.0491 $[\text{M}]^+$; found: 422.0485.

9-Nonyl-3-iodo-6-nitrocarbazole (C₉-4) – The iodo compound **C₉-4** was prepared as a yellow solid following the same procedure as **C₆-4** in 92% yield from **C₉-3**. ^1H NMR (500 MHz, chloroform-*d*) δ / ppm = 8.99 (d, $J = 2.2$ Hz, 1H), 8.50 (d, $J = 1.7$ Hz, 1H), 8.42 (dd, $J = 9.1, 2.2$ Hz, 1H), 7.84 (dd, $J = 8.6, 1.7$ Hz, 1H), 7.43 (d, $J = 9.0$ Hz, 1H), 7.28 (d, $J = 1.9$ Hz, 2H), 4.34 (t, $J = 7.3$ Hz, 2H), 1.89 (p, $J = 7.3$ Hz, 2H), 1.48 – 1.20 (m, 14H), 0.88 (t, $J = 7.0$ Hz, 3H). ^{13}C NMR (125 MHz, chloroform-*d*) δ / ppm = 143.35, 140.97, 140.81, 135.65, 129.88, 125.20, 122.16,

121.24, 117.51, 111.63, 108.55, 83.32, 43.75, 31.76, 29.37, 29.28, 29.15, 28.85, 27.18, 22.60, 14.06. HRMS (EI) calculated for $C_{21}H_{25}IN_2O_2 + H$: 465.1034 $[M+H]^+$; found: 465.1033.

3-Azido-9-hexyl-6-iodocarbazole (C₆-5) – A mixture of **C₆-4** (2.13 g, 5.04 mmol) and $SnCl_2 \cdot 2H_2O$ (5.70 g, 25.25 mmol) in EtOAc (50 mL) and EtOH (50 mL) was heated at reflux overnight. After cooling to room temperature, the reaction mixture was poured into an aqueous solution of Na_2CO_3 and stirred for 2 hours, then extracted with EtOAc. The organic phase was dried with $MgSO_4$, filtered, and concentrated in vacuo to give the amino carbazole intermediate as a light brown solid. This intermediate and *p*-toluenesulfonic acid monohydrate (2.88 g, 15.12 mmol) were mixed in THF (50 ml) and cooled to 0 °C (ice bath) resulting in a dark brown slurry. A solution of $NaNO_2$ (0.38 g, 5.5 mmol) in water (2 mL) was added dropwise, and the mixture was stirred for 1 hour. A solution of NaN_3 (0.39 g, 6 mmol) in water (2 mL) was added drop-wise, followed by stirring for 1 hour at 0°C. The mixture was warmed to room temperature and stirred for an additional 30 min. The mixture was basified with a NaOH solution (1 M, 25 mL) and extracted with EtOAc. The organic phase was dried with $MgSO_4$ and concentrated in vacuo to give **C₆-5** as a light brown solid (2.01 g, 4.8 mmol, 95% yield). 1H NMR (500 MHz, chloroform-*d*) δ / ppm = 8.33 (d, J = 1.6 Hz, 1H), 7.68 (dd, J = 8.6, 1.7 Hz, 1H), 7.64 (d, J = 2.2 Hz, 1H), 7.32 (d, J = 8.7 Hz, 1H), 7.15 (d, J = 8.6 Hz, 1H), 7.12 (dd, J = 8.7, 2.2 Hz, 1H), 4.21 (t, J = 7.2 Hz, 2H), 1.79 (q, J = 7.3 Hz, 2H), 1.41 – 1.11 (m, 6H), 0.83 (t, J = 6.9 Hz, 3H). ^{13}C NMR (125 MHz, chloroform-*d*) δ / ppm = 140.12, 137.94, 134.41, 131.64, 129.40, 124.49, 122.42, 117.98, 110.98, 110.36, 109.92, 81.23, 43.34, 31.49, 28.86, 26.88, 22.49, 13.96. HRMS (EI) calculated for $C_{18}H_{19}IN_4$: 418.0654 $[M]^+$; found: 418.0659.

3-Azido-6-iodo-9-nonylcarbazole (C₉-5) – Azido carbazole **C₉-5** was prepared as a brown solid following the same procedure as **C₆-5** in 93% yield from **C₉-4**. 1H NMR (500 MHz, chloroform-

d) δ / ppm = 8.34 (d, J = 1.6 Hz, 1H), 7.71 (dd, J = 8.6, 1.7 Hz, 1H), 7.65 (d, J = 2.2 Hz, 1H), 7.34 (s, 1H), 7.20 – 7.12 (m, 2H), 4.22 (t, J = 7.2 Hz, 2H), 1.83 (p, J = 7.3 Hz, 2H), 1.41 – 1.18 (m, 12H), 0.90 (t, J = 7.0 Hz, 3H). ^{13}C NMR (125 MHz, chloroform-*d*) δ / ppm = 140.09, 137.91, 134.39, 131.60, 129.36, 124.47, 122.39, 117.96, 110.97, 110.33, 109.91, 81.26, 43.32, 31.80, 29.43, 29.35, 29.21, 28.90, 27.23, 22.64, 14.10. HRMS (EI) calculated for $\text{C}_{21}\text{H}_{25}\text{IN}_4$: 460.1124 $[\text{M}]^+$; found: 460.1107.

3-Azido-6-ethynyl-9-hexylcarbazole (C6-6) – To a degassed solution of **C6-5** (2.01 g, 4.8 mmol) and diisopropylamine (3.4 mL, 24 mmol) in THF (50 mL) was added $[\text{PdCl}_2(\text{PPh}_3)_2]$ (70 mg, 0.1 mmol), CuI (45 mg, 0.24 mmol), and trimethylsilylacetylene (1 mL, 7.2 mmol). The reaction mixture was stirred under an argon atmosphere for 40 min and quenched with an aqueous solution of NH_4Cl (25 mL). The mixture was extracted with EtOAc, and the organic phase was dried with MgSO_4 , filtered, and concentrated in vacuo. The resulting viscous oil mixture was subjected to column chromatography on silica gel with hexanes/EtOAc 97:3 to give a light brown, viscous oil. This intermediate was then dissolved in THF (20 mL), MeOH (20 mL), and a saturated K_2CO_3 solution in MeOH (5 mL). The mixture stirred for 1 hour, was quenched with a saturated NH_4Cl solution (25 mL) and extracted with CH_2Cl_2 , then dried with MgSO_4 , filtered, and finally concentrated in vacuo to give **C6-6** as a light brown solid (1.30 g, 4.1 mmol, 85% yield). ^1H NMR (500 MHz, chloroform-*d*) δ / ppm = 8.19 (d, J = 1.5 Hz, 1H), 7.68 (d, J = 2.2 Hz, 1H), 7.57 (dd, J = 8.5, 1.6 Hz, 1H), 7.34 (d, J = 8.7 Hz, 1H), 7.30 (d, J = 8.5 Hz, 1H), 7.12 (dd, J = 8.7, 2.3 Hz, 1H), 4.23 (t, J = 7.3 Hz, 2H), 3.04 (s, 1H), 1.82 (q, J = 7.4 Hz, 2H), 1.41 – 1.06 (m, 6H), 0.83 (t, J = 7.0 Hz, 3H). ^{13}C NMR (125 MHz, chloroform-*d*) δ / ppm = 140.83, 138.36, 131.73, 130.16, 124.88, 123.29, 121.92, 117.77, 112.26, 110.44, 109.99, 108.94, 84.73, 75.35, 43.39, 31.50, 28.91, 26.89, 22.50, 13.96. HRMS (EI) calculated for $\text{C}_{20}\text{H}_{20}\text{N}_4$: 316.1688 $[\text{M}]^+$; found: 316.1703.

3-Azido-6-ethynyl-9-nonylcarbazole (C9-6) – Alkynyl carbazole **C9-6** was prepared as a tan solid following the same procedure as **C6-6** in 90% yield from **C9-5**. ^1H NMR (400 MHz, chloroform-*d*) δ / ppm = 8.18 (d, J = 1.5 Hz, 1H), 7.67 (d, J = 2.2 Hz, 1H), 7.57 (dd, J = 8.5, 1.6 Hz, 1H), 7.37 – 7.28 (m, 2H), 7.12 (dd, J = 8.7, 2.2 Hz, 1H), 4.22 (t, J = 7.2 Hz, 2H), 3.04 (s, 1H), 1.81 (p, J = 7.2 Hz, 2H), 1.44 – 1.09 (m, 12H), 0.83 (t, J = 6.8 Hz, 3H). ^{13}C NMR (125 MHz, chloroform-*d*) δ / ppm = 140.84, 138.37, 131.73, 130.16, 124.88, 123.30, 121.93, 117.77, 112.27, 110.44, 110.01, 108.95, 84.74, 75.35, 43.40, 31.78, 29.42, 29.34, 29.19, 28.94, 27.23, 22.61, 14.07. HRMS (EI) calculated for $\text{C}_{23}\text{H}_{26}\text{N}_4$: 358.2163 [M] $^+$; found: 358.2151.

Trihexyl-tricarbazolo-triazolophane (TC-6) – To a degassed solution of $\text{CuSO}_4 \cdot 5\text{H}_2\text{O}$ (100 mg, 0.41 mmol), sodium ascorbate (160 mg, 0.82 mmol) and tris[(1-benzyl-1H-1,2,3-triazol-4-yl)methyl]amine (TBTA, 220 mg, 0.41 mmol) in THF (50 mL), EtOH (25 mL), and water (25 mL), a solution of **C6-6** (1.3 g, 4.1 mmol) in THF (25 mL) and EtOH (25 mL) was added dropwise over 6 h at 70 °C. The reaction mixture was stirred for an additional 2 h, then cooled to room temperature. Organic solvents (THF and EtOH) were removed in vacuo. The mixture was extracted with CHCl_3 , and the organic phase was washed with NH_4Cl solution (75 mL) and dried with MgSO_4 , filtered, and concentrated in vacuo. The resulting solid mixture was subjected to column chromatography (SiO_2) using an eluent gradient from CHCl_3 to CHCl_3 :EtOAc 95:5. The product was obtained as a light yellow solid (2.51 g, 2.65 mmol, 65% yield). ^1H NMR (500 MHz, chloroform-*d*) δ / ppm = 8.69 (s, 1H), 8.22 (s, 1H), 8.14 (d, J = 8.2 Hz, 1H), 8.10 (d, J = 8.6 Hz, 1H), 8.07 (s, 1H), 7.17 (d, J = 8.4 Hz, 2H), 4.08 (s, 2H), 1.87 – 1.69 (m, 2H), 1.42 – 1.12 (m, 6H), 0.85 (t, J = 6.9 Hz, 3H). ^{13}C NMR (125 MHz, chloroform-*d*) δ / ppm = 149.66, 140.82, 139.91, 129.26, 123.97, 122.55, 122.42, 121.90, 118.35, 117.67, 117.54, 110.59, 109.37, 109.20, 43.42,

31.60, 29.22, 26.96, 22.57, 14.03. HRMS (ESI) calculated for $C_{60}H_{60}N_{12} \cdot PF_6$: 1093.4706 [M + PF_6]⁻; found: 1093.4758.

Trinonyl-tricarbazolo-triazolophane (TC-9) – Macrocyclic **TC-9** was prepared as an off-white solid following the same procedure as **TC-6** in 70% yield from **C9-6**. ¹H NMR (600 MHz, chloroform-*d*) δ / ppm = 8.73 (s, 1H), 8.27 (s, 1H), 8.18 (d, *J* = 8.3 Hz, 1H), 8.15 (d, *J* = 8.4 Hz, 1H), 8.11 (s, 1H), 7.21 (d, *J* = 8.6 Hz, 2H), 4.12 (t, *J* = 7.3 Hz, 2H), 1.81 – 1.75 (m, 2H), 1.44 – 1.14 (m, 12H), 0.85 – 0.79 (t, *J* = 7.03 Hz, 3H). ¹³C NMR (125 MHz, chloroform-*d*) δ / ppm = 49.70, 140.86, 139.95, 129.30, 124.03, 122.58, 122.45, 121.92, 118.38, 117.72, 110.64, 109.43, 109.26, 43.45, 31.78, 29.71, 29.40, 29.26, 29.19, 27.31, 22.61, 14.07. HRMS (ESI) calculated for $C_{69}H_{78}N_{12} \cdot PF_6$: 1219.6121 [M + PF_6]⁻; found: 1219.6109.

Acknowledgements

We thank the National Science Foundation (DMR 1533988) for support. We also thank Xinfeng (Frank) Gao at Indiana University for help with the NMR spectroscopy.

References

- [1] a) J. A. A. W. Elemans, A. E. Rowan, R. J. M. Nolte, *J. Mater. Chem.* **2003**, *13*, 2661-2670; b) C. Rest, R. Kandanelli, G. Fernandez, *Chem. Soc. Rev.* **2015**, *44*, 2543-2572; c) E. Yashima, N. Ousaka, D. Taura, K. Shimomura, T. Ikai, K. Maeda, *Chem. Rev.* **2016**, *116*, 13752-13990.
- [2] a) M. J. Webber, E. A. Appel, E. W. Meijer, R. Langer, *Nature Materials* **2015**, *15*, 13; b) J.-M. Lehn, *Angew. Chem. Int. Ed.* **2015**, *54*, 3276-3289; *Angew. Chem.* **2015**, *127*, 3326-3340; c) A. Wang, W. Shi, J. Huang, Y. Yan, *Soft Matter* **2016**, *12*, 337-357.
- [3] a) D. L. Caulder, C. Bruckner, R. E. Powers, S. Konig, T. N. Parac, J. A. Leary, K. N. Raymond, *J. Am. Chem. Soc.* **2001**, *123*, 8923-8938; b) R. M. Yeh, J. Xu, G. Seeber, K. N. Raymond, *Inorg. Chem.* **2005**, *44*, 6228-6239; c) P. Mal, B. Breiner, K. Rissanen, J. R. Nitschke, *Science* **2009**, *324*, 1697-1699; d) T. Liu, Y. Liu, W. Xuan, Y. Cui, *Angew. Chem. Int. Ed.* **2010**, *49*, 4121-4124; *Angew. Chem.* **2010**, *122*, 4215-4218.

- [4] a) S. Roche, C. Haslam, S. L. Heath, J. A. Thomas, *Chem. Commun.* **1998**, 1681-1682; b) J. Mosquera, B. Szyszko, S. K. Y. Ho, J. R. Nitschke, *Nat. Commun.* **2017**, *8*, 14882.
- [5] a) W. T. S. Huck, F. C. J. M. Van Veggel, B. L. Kropman, D. H. A. Blank, E. G. Keim, M. M. A. Smithers, D. N. Reinhoudt, *J. Am. Chem. Soc.* **1995**, *117*, 8293-8294; b) D. K. Chand, K. Biradha, M. Fujita, S. Sakamoto, K. Yamaguchi, *Chem. Commun.* **2002**, 2486-2487; c) D. Fujita, Y. Ueda, S. Sato, H. Yokoyama, N. Mizuno, T. Kumasaka, M. Fujita, *Chem* **2016**, *1*, 91-101.
- [6] a) M. M. J. Smulders, I. A. Riddell, C. Browne, J. R. Nitschke, *Chem. Soc. Rev.* **2013**, *42*, 1728-1754; b) T. R. Cook, P. J. Stang, *Chem. Rev.* **2015**, *115*, 7001-7045.
- [7] a) M. Arunachalam, P. Ghosh, *Chem. Commun.* **2011**, *47*, 8477-8492; b) N. G. White, M. J. MacLachlan, *Cryst. Growth Des.* **2015**, *15*, 5629-5636.
- [8] a) B. Hasenknopf, J.-M. Lehn, B. O. Kneisel, G. Baum, D. Fenske, *Angew. Chem. Int. Ed.* **1996**, *35*, 1838-1840; *Angew. Chem.* **1996**, *108*, 1987-1990; b) J.-F. Ayme, J. E. Beves, D. A. Leigh, R. T. McBurney, K. Rissanen, D. Schultz, *Nat. Chem* **2011**, *4*, 15; c) F. Cui, S. Li, C. Jia, J. S. Mathieson, L. Cronin, X.-J. Yang, B. Wu, *Inorg. Chem.* **2012**, *51*, 179-187; d) I. A. Riddell, M. M. J. Smulders, J. K. Clegg, Y. R. Hristova, B. Breiner, J. D. Thoburn, J. R. Nitschke, *Nat. Chem* **2012**, *4*, 751; e) M. Han, D. M. Engelhard, G. H. Clever, *Chem. Soc. Rev.* **2014**, *43*, 1848-1860.
- [9] a) J. Keegan, P. E. Kruger, M. Nieuwenhuyzen, J. O'Brien, N. Martin, *Chem. Commun.* **2001**, 2192-2193; b) S. J. Coles, J. G. Frey, P. A. Gale, M. B. Hursthouse, M. E. Light, K. Navakhun, G. L. Thomas, *Chem. Commun.* **2003**, 568-569; c) U.-I. Kim, J.-m. Suk, V. R. Naidu, K.-S. Jeong, *Chem. Eur. J.* **2008**, *14*, 11406-11414; d) H. Juwarker, K.-S. Jeong, *Chem. Soc. Rev.* **2010**, *39*, 3664-3674; e) J.-i. Kim, H. Juwarker, X. Liu, M. S. Lah, K.-S. Jeong, *Chem. Commun.* **2010**, *46*, 764-766; f) S. Li, C. Jia, B. Wu, Q. Luo, X. Huang, Z. Yang, Q.-S. Li, X.-J. Yang, *Angew. Chem. Int. Ed.* **2011**, *50*, 5721-5724; *Angew. Chem.* **2011**, *123*, 5839-5842; g) J.-m. Suk, V. R. Naidu, X. Liu, M. S. Lah, K.-S. Jeong, *J. Am. Chem. Soc.* **2011**, *133*, 13938-13941.
- [10] a) B. Wu, F. Cui, Y. Lei, S. Li, N. de Sousa Amadeu, C. Janiak, Y.-J. Lin, L.-H. Weng, Y.-Y. Wang, X.-J. Yang, *Angew. Chem. Int. Ed.* **2013**, *52*, 5096-5100; *Angew. Chem.* **2013**, *125*, 5200-5204; b) D. Yang, J. Zhao, Y. Zhao, Y. Lei, L. Cao, X.-J. Yang, M. Davi, N. de Sousa Amadeu, C. Janiak, Z. Zhang, Y.-Y. Wang, B. Wu, *Angew. Chem. Int. Ed.* **2015**, *54*, 8658-8661; *Angew. Chem.* **2015**, *127*, 8782-8785; c) D. Yang, J. Zhao, L. Yu, X. Lin, W. Zhang, H. Ma, A. Gogoll, Z. Zhang, Y. Wang, X.-J. Yang, B. Wu, *J. Am. Chem. Soc.* **2017**, *139*, 5946-5951.
- [11] a) F. Weinhold, R. A. Klein, *Angew. Chem. Int. Ed.* **2014**, *53*, 11214-11217; *Angew. Chem.* **2014**, *126*, 11396-11399; b) F. Weinhold, R. A. Klein, *Angew. Chem. Int. Ed.* **2015**, *54*, 2600-2602; *Angew. Chem.* **2015**, *127*, 2636-2638.; c) G. Frenking, G. F. Caramori, *Angew. Chem. Int. Ed.* **2015**, *54*, 2596-2599; *Angew. Chem.* **2015**, *127*, 2632-2635; d) J. S. McNally, X. P. Wang, C. Hoffmann, A. D. Wilson, *Chem. Commun.* **2017**, *53*, 10934-10937; e) C. Wang, Y. Fu, L. Zhang, D. Danovich, S. Shaik, Y. Mo, *J. Comput. Chem.* **2018**, *39*, 481-487.
- [12] a) I. Mata, I. Alkorta, E. Molins, E. Espinosa, *ChemPhysChem* **2012**, *13*, 1421-1424; b) I. Mata, I. Alkorta, E. Molins, E. Espinosa, *Chem. Phys. Lett.* **2013**, *555*, 106-109; c) I. Mata, E. Molins, I. Alkorta, E. Espinosa, *J. Phys. Chem. A* **2015**, *119*, 183-194.
- [13] Q. He, P. Tu, J. L. Sessler, *Chem* **2018**, *4*, 46-93.

- [14] a) E. M. Fatila, E. B. Twum, A. Sengupta, M. Pink, J. A. Karty, K. Raghavachari, A. H. Flood, *Angew. Chem. Int. Ed.* **2016**, *55*, 14057-14062; *Angew. Chem.* **2016**, *128*, 14263–14268; b) E. M. Fatila, E. B. Twum, J. A. Karty, A. H. Flood, *Chem. Eur. J.* **2017**, *23*, 10652-10662.
- [15] a) H.-Y. Gong, B. M. Rambo, E. Karnas, V. M. Lynch, J. L. Sessler, *Nat. Chem.* **2010**, *2*, 406; b) H.-Y. Gong, B. M. Rambo, E. Karnas, V. M. Lynch, K. M. Keller, J. L. Sessler, *J. Am. Chem. Soc.* **2011**, *133*, 1526-1533; c) N. L. Bill, D.-S. Kim, S. K. Kim, J. S. Park, V. M. Lynch, N. J. Young, B. P. Hay, Y. Yang, E. V. Anslyn, J. L. Sessler, *Supramol. Chem.* **2012**, *24*, 72-76; d) H.-Y. Gong, B. M. Rambo, V. M. Lynch, K. M. Keller, J. L. Sessler, *J. Am. Chem. Soc.* **2013**, *135*, 6330-6337; e) D. Mungalpara, A. Valkonen, K. Rissanen, S. Kubik, *Chem. Sci.* **2017**, *8*, 6005-6013; f) D. Mungalpara, H. Kelm, A. Valkonen, K. Rissanen, S. Keller, S. Kubik, *Org. Biomol. Chem.* **2017**, *15*, 102-113; g) Q. He, M. Kelliher, S. Bähring, V. M. Lynch, J. L. Sessler, *J. Am. Chem. Soc.* **2017**, *139*, 7140-7143.
- [16] a) W. Zhao, B. Qiao, C.-H. Chen, A. H. Flood, *Angew. Chem. Int. Ed.* **2017**, *56*, 13083-13087; *Angew. Chem.* **2017**, *129*, 13263–13267; b) E. M. Fatila, M. Pink, E. B. Twum, J. A. Karty, A. H. Flood, *Chem. Sci.* **2018**, *9*, 2863-2872.
- [17] a) S. Lee, B. E. Hirsch, Y. Liu, J. R. Dobscha, D. W. Burke, S. L. Tait, A. H. Flood, *Chem. Eur. J.* **2016**, *22*, 560-569; b) S. Jin, S.-i. Kato, Y. Nakamura, *Chem. Lett.* **2016**, *45*, 869-871.
- [18] a) R. Schmidt, S. Uemura, F. Würthner, *Chem. Eur. J.* **2010**, *16*, 13706-13715; b) G. Charalambidis, E. Georgilis, M. K. Panda, C. E. Anson, A. K. Powell, S. Doyle, D. Moss, T. Jochum, P. N. Horton, S. J. Coles, M. Linares, D. Beljonne, J.-V. Naubron, J. Conradt, H. Kalt, A. Mitraki, A. G. Coutsolelos, T. S. Balaban, *Nat. Commun.* **2016**, *7*, 12657.
- [19] a) D. Schultz, G. Bernardinelli, D. Gerard, J. R. Nitschke, *J. Am. Chem. Soc.* **2004**, *126*, 16538-16543; b) M. Hutin, J. Nitschke, *Chem. Commun.* **2006**, 1724-1726; c) T. D. Nguyen, S. C. Glotzer, *Small* **2009**, *5*, 2092-2098.
- [20] a) K. Choi, A. D. Hamilton, *J. Am. Chem. Soc.* **2003**, *125*, 10241-10249; b) Y. Li, M. Pink, J. A. Karty, A. H. Flood, *J. Am. Chem. Soc.* **2008**, *130*, 17293-17295; c) Y. Li, A. H. Flood, *Angew. Chem. Int. Ed.* **2008**, *47*, 2649-2652; *Angew. Chem.* **2008**, *120*, 2689–2692; d) Y. Hua, Y. Liu, C.-H. Chen, A. H. Flood, *J. Am. Chem. Soc.* **2013**, *135*, 14401-14412.
- [21] R. B. Martin, *Chem. Rev.* **1996**, *96*, 3043-3064.
- [22] W. Zhang, J. S. Moore, *Angew. Chem. Int. Ed.* **2006**, *45*, 4416-4439; *Angew. Chem.* **2006**, *118*, 4524–4548.
- [23] Y. Liu, A. Sengupta, K. Raghavachari, A. H. Flood, *Chem* **2017**, *3*, 411-427.
- [24] a) O. B. Berryman, A. C. Sather, B. P. Hay, J. S. Meisner, D. W. Johnson, *J. Am. Chem. Soc.* **2008**, *130*, 10895-10897; b) Y. R. Hristova, M. M. J. Smulders, J. K. Clegg, B. Breiner, J. R. Nitschke, *Chem. Sci.* **2011**, *2*, 638-641; c) K. P. McDonald, R. O. Ramabhadran, S. Lee, K. Raghavachari, A. H. Flood, *Org. Lett.* **2011**, *13*, 6260-6263; d) S. Lee, C.-H. Chen, A. H. Flood, *Nat. Chem.* **2013**, *5*, 704; e) M. A. Yawer, V. Havel, V. Sindelar, *Angew. Chem. Int. Ed.* **2015**, *54*, 276-279; *Angew. Chem.* **2015**, *127*, 278–281.
- [25] L. Alderighi, P. Gans, A. Ienco, D. Peters, A. Sabatini, A. Vacca, *Coord. Chem. Rev.* **1999**, *184*, 311-318.
- [26] T. Nagai, S. Prakongpan, *Chem. Pharm. Bull.* **1984**, *32*, 340-343.
- [27] O. Köhl, *Phosphorus-31 NMR Spectroscopy*, Springer-Verlag, Berlin, **2009**.
- [28] B. Qiao, B. E. Hirsch, S. Lee, M. Pink, C.-H. Chen, B. W. Laursen, A. H. Flood, *J. Am. Chem. Soc.* **2017**, *139*, 6226-6233.

- [29] G. A. Jeffrey, *An Introduction to Hydrogen Bonding*, Oxford University Press, New York, **1997**.
- [30] F. Weinhold, *Angew. Chem. Int. Ed.* **2017**, *56*, 14577-14581; *Angew. Chem.* **2017**, *129*, 14769–14773.
- [31] a) J. Sartorius, H.-J. Schneider, *Chem. Eur. J.* **1996**, *2*, 1446-1452; b) F. H. Beijer, R. P. Sijbesma, H. Kooijman, A. L. Spek, E. W. Meijer, *J. Am. Chem. Soc.* **1998**, *120*, 6761-6769; c) C. Schmuck, W. Wienand, *Angew. Chem. Int. Ed.* **2001**, *40*, 4363-4369; *Angew. Chem.* **2001**, *113*, 4493-4499.
- [32] a) S. A. Arnstein, C. D. Sherrill, *Phys. Chem. Chem. Phys.* **2008**, *10*, 2646-2655; b) E. G. Hohenstein, C. D. Sherrill, *J. Phys. Chem. A* **2009**, *113*, 878-886; c) C. R. Martinez, B. L. Iverson, *Chem. Sci.* **2012**, *3*, 2191-2201.
- [33] Y. An, J. W. G. Bloom, S. E. Wheeler, *J. Phys. Chem. B* **2015**, *119*, 14441-14450.
- [34] G. Dey, A. Gupta, T. Mukherjee, P. Gaur, A. Chaudhary, S. K. Mukhopadhyay, C. K. Nandi, S. Ghosh, *ACS Appl. Mater. Interfaces* **2014**, *6*, 10231.
- [35] A. D. Finke, D. E. Gross, A. Han, J. S. Moore, *J. Am. Chem. Soc.* **2011**, *133*, 14063.